Biosensors and Bioelectronics 45 (2013) 108–113

Contents lists available at SciVerse ScienceDirect

Biosensors and Bioelectronics

journal homepage: www.elsevier.com/locate/bios

A novel electrically magnetic-controllable electrochemical biosensor for the ultra sensitive and specific detection of attomolar level oral cancer-related microRNA

ZongWen Wang [a], Jing Zhang [b], Ying Guo [a], XiaoYan Wu [a], WeiJuan Yang [a], LiangJun Xu [a], JingHua Chen [c,*], FengFu Fu [a,*]

[a] Key Lab of Analysis and Detection for Food Safety of Ministry of Education, Fujian Provincial Key Lab of Analysis and Detection for Food Safety, Department of Chemistry, Fuzhou University, Fuzhou, Fujian 350108, China
[b] Department of Chemistry and Biology, Faculty of Life Science, Fujian Agriculture and Forestry University, Fuzhou, Fujian 350002, China
[c] Department of Pharmaceutical Analysis, Faculty of Pharmacy, Fujian Medical University, Fuzhou, Fujian 350004, China

ARTICLE INFO

Article history:
Received 10 December 2012
Received in revised form
30 January 2013
Accepted 4 February 2013
Available online 13 February 2013

Keywords:
RNA biosensor
Magnetic-controllable electrochemical biosensor
miRNA
Oral cancer
Saliva

ABSTRACT

Non-invasive early diagnosis of oral cancer is the most effective means to reduce mortality rate from this disease. In this paper, we described a novel magnetic-controllable electrochemical RNA biosensor for the ultra sensitive and specific detection of oral cancer-related microRNA (miRNA) based on a home-made electrically magnetic-controllable gold electrode. The electrically magnetic-controllable gold electrode combined the merits of heated electrode and magnetic electrode, has notable advantage such as that the strength and direction of the magnetic field and the temperature of the electrode's surface can be easily regulated. The advantage of electrically magnetic-controllable gold electrode, as well as the utilization of "junction-probe" strategy and magnetic beads (MBs)-based enzymatic catalysis amplification, make the biosensor has ultra-high sensitivity and discrimination ability even for the detection of similar miRNAs. It can be used to detect as low as 0.22 aM (2.2×10^{-19} M) of oral cancer-related miRNA with a recovery of 93–108% and a RSD < 6 (n=5). The high sensitivity and selectivity, as well as the easiness of fabrication, operational convenience, short analysis time, good stability and re-usability, make the biosensor a promising alternative for the early point-of-care diagnosis of oral cancer. The success of the biosensor also leads to a great potential in the development of biosensor for the early diagnosis of other diseases.

1. Introduction

Oral squamous cell carcinoma (OSCC) is the 11th most common cancer worldwide, it accounts for more than 90% of total oral cancer (Brinkman and Wong, 2006). Approximately 50–70% of OSCC patients died within 5 years after OSCC was diagnosed, and the mortality rate did not decrease over the past years (Zetola and Pilcher, 2007). The key factor for the high mortality rate is that most OSCC are asymptomatic lesions initially, which makes it can not be diagnosed or treated in the initial stage. Therefore, the development of the early point-of-care diagnostic method of OSCC, which is characterized as ultra-sensitive, specific, non-invasive and cost-effective, is of great significance to increase the survival rate of OSCC patients (von Lode, 2005; Warsinke, 2009). Along this direction, saliva has been used as a diagnostic medium for OSCC, and it was reported that some proteins, DNA and mRNA in saliva can be used as biomarker for the detection of OSCC (Chai and Grandis, 2006; Hu et al., 2008). Recently, two miRNAs (miR-200a and miR-125a) are found differentially expressed in the saliva of the OSCC patients in comparison with healthy persons (Park et al., 2009). These two miRNAs is a class of short (19–24 bases) endogenous non-coding RNAs that mediate post-transcriptional gene regulation by base pairing to the 3'untranslated region of messenger RNAs. It was reported that these two miRNAs seem more accurately cluster different types of solid tumors than mRNA, and the fold change in these two miRNAs between cancer cells and normal cells is relatively great (Lu et al., 2005; Park et al., 2009). All above finding suggested that the detection of miRNA in saliva may be used as a non-invasive and rapid diagnostic tool for the early diagnosis of OSCC.

So far, various strategies have been developed for the detection of miRNA, such as real-time quantitative PCR (Chen, et al. 2005; Raymond et al., 2005), locked nucleic acid-based northern blot (Válóczi et al., 2004), microarray or MBs-based flowcytometry

* Corresponding authors. Tel./fax: +86 591 22866135.
E-mail addresses: cjh_huaxue@126.com (J. Chen), fengfu@fzu.edu.cn (F. Fu).

0956-5663/$ - see front matter © 2013 Elsevier B.V. All rights reserved.
http://dx.doi.org/10.1016/j.bios.2013.02.007

and so on (Chen et al., 2008a; Liu et al., 2008). However, these strategies suffer from one or more of following disadvantages: relatively long analysis time, inadequate sensitivity and stability, higher assay cost, and over- or under-estimation of the concentration of target RNA since certain alleles amplify better than others under PCR conditions. In an effort to resolve the aforementioned limitations of above methods, some alternative detection methods such as hybridization-based biosensors have been developed (Gao and Peng, 2011; Peng and Gao, 2011). Owing to the fact that electrochemical detector is simple, portable, sensitive, fast response and low cost, electrochemical biosensors have been recognized to be the most promising way for the early diagnostic purpose (Kwon and Bard, 2012; Zhang et al., 2010). To date, various sensing strategies have been developed to improve the sensitivity and specificity of electrochemical RNA biosensors (Gao and Peng, 2011; Mascini et al., 2012; Peng and Gao, 2011). However, due to the facts of low concentration, complex matrix and intrinsic properties of miRNA such as short size, sequence similarity among family members and susceptibility to degradation, the conventional electrochemical biosensor do not meet the early diagnostic requirement of sensitively and specifically detecting ultra-trace miRNA in saliva. So, it is very significant to develop a novel electrochemical biosensor for the ultra sensitive and specific detection of salivary miRNA in order to provide a reliable approach for the non-invasive early diagnosis of OSCC.

Junction-probe is a novel DNA detection technique reported recently (Nakayama et al., 2008; Zhang et al., 2009). It operates via a concept called template-enhanced hybridization processes (TeHyP), which encompasses a design strategy whereby two probes that do not hybridize to each other at a specific temperature can be made to anneal to each other in the presence of a template (target) via the formation of "Y" junction structure. This technique can amplify DNA detection signal under isothermal conditions and improve the specificity for the detection of single-base mismatch. Surprisingly, Guo and his colleagues found that RNA can also self-assemble into a thermodynamically stable three-way junction structure (Shu et al., 2011). Stimulated by their research, we herein developed an ultra sensitive and specific magnetic-controllable electrochemical RNA biosensor for the determination of attomolar OSCC-related miRNA (hsa-miR-200a) in saliva based on an electrically magnetic-controllable gold electrode with MBs-based enzymatic catalysis amplification and junction-probe strategy. The combination of the electrically magnetic-controllable electrode, junction probe strategy and MBs-based enzyme amplification provides an ultra-high sensitivity and specificity for the miRNA detection, which will meet the requirement of the early point-of-care diagnosis of OSCC.

2. Experimental section

2.1. Reagent and materials

All oligonucleotides were synthesized by TaKaRa biotechnology Co. Ltd. (Dalian, China), and their base sequences were illustrated in Table S1 (see supporting information). The stock standard solution of miRNA (about 1 μM) was prepared by dissolving miRNA in sterile DEPC-treated Milli-Q water and its concentration was accurately quantified by OD260 based on their individual absorption coefficients. More dilute standard solutions of miRNA were prepared by serially diluting the stock standard solution (each diluted 10-fold) to the desired concentration with hybridization buffer solution. Streptavidin-modified MBs (1 μm, 10 mg/mL) were purchased from Dynal Biotech ASA. Streptavidin-HRP (horseradish peroxidase) was purchased from Sigma (Spain) and used as received. TMB (3,3′,5,5′-tetramethylbenzidine sulfate)/H_2O_2 solution was purchased from Neogen Corporation (USA), and the ethylenediaminetetraacetic acid (EDTA) were purchased from Sigma-Aldrich (St. Louis, MO, USA). Tris-(hydroxymethyl) aminomethane(Tris) was purchased from Cxbio Biotechnology Co. Ltd. (Denmark). All chemicals are of analytical grade.

Stock solutions of streptavidin-HRP (10 μg/mL) were prepared in a saline 0.01 M phosphate buffer solution in which containing 0.05% Tween 20, 0.138 M NaCl and 0.0027 M KCl (PBST, pH 7.4). RNA immobilization buffer was the mixture of 10 mM Tris, 1.0 mM EDTA, 0.01% Tween 20 and 1 M NaCl (pH 7.5). Hybridization buffer was the mixture of 50 mM Tris, 0.01% Tween 20 and 20 mM NaCl (pH 7.4). Washing buffer solution was 0.1 M NaCl, 0.05% Tween 20 and 10 mM PB solution (pH 7.4). All solutions were prepared with Milli-Q water (18.2 MΩ/cm).

2.2. Fabrication and pretreatment of the electrically magnetic-controllable gold working electrode

The electrically magnetic-controllable gold working electrode used in the experiment is similar to that previously reported (Zhang et al., 2013). The structure of the working electrode was shown in Figure S1 (see supporting information). A piece of gold circular plate (thickness 1 mm, diameter 3 mm) was directly fixed on the end of a iron rod (length 5 cm, diameter 3 mm) by welding, and the iron rod was enlaced with varnished wire (internal diameter 0.10 mm) to form coil from the end with a height of 3 cm and a electric resistance of 22 Ω. The outside of the electrode was finally sealed with polytetrafluoroethylene. Two ends of the coil were then connected to the outlets of a voltage-controllable DC power supply (0–10 V). The magnetic force of the electrode and the temperature of the electrode's surface can be precisely controlled by adjusting the voltage.

Before use, the electrode was firstly polished to obtain mirror surface with 0.05 μm alumina powder, followed by sonication in ethanol and water for 5 min respectively. The working electrode was then electrochemically cleaned to remove any remaining impurities (Fan et al., 2003). After drying with nitrogen, the electrode was immediately used for electrochemical measurements.

2.3. Capture probe self-assembly and hybridization on the surface of MBs

Capture probe self-assembly was carried out by a procedure recommended by Dynal Biotech ASA (Oslo, Norway). About 50 μL of streptavidin-modified MBs was added into a 2.0 mL centrifuge vial. Under the magnetic field, the MBs was washed three times with immobilization buffer and re-suspended in 125 μL of the same buffer in which containing 2.5 μM of biotinylated capture probe (C_p). The mixture was incubated for 30 min at 37 °C to immobilize C_p on the surface of MBs. Subsequently, the C_p-modified MBs were washed three times with hybridization buffer and re-suspended in 100 μL of the same buffer solution. Accordingly, 40 μL of the mixture of signal probe (S_p) and complementary target miRNA (T) (S_p was pre-annealed with T at 30 °C for 30 min in hybridization buffer solution) was added into 8 μL of C_p-modified MBs and the mixture was incubated for 2 h at 37 °C to complete hybridization. Then, the resulting hybrid-attached MBs were extensively rinsed with washing buffer solution to remove the nonspecific RNA adsorption under the magnetic field. Finally, 40 μL of 10 μg/ml streptavidin-HRP was added to the hybrid-attached MBs with gentle mixing for 30 min at 37 °C. The resulting HRP-tagged MBs were washed five times (for 5 min each) under the magnetic field with 100 μL of washing

buffer solution, and final HRP-tagged MBs were used for the electrochemical measurements in the TMB/H_2O_2 solution.

2.4. Electrochemical measurements

All electrochemical measurements were performed with a CHI-660D electrochemical workstation (CH Instrument, USA). The electrochemical system consisted of the electrically magnetic-controllable gold electrode as working electrode, a platinum wire as the auxiliary electrode, and a Ag/AgCl as reference electrode. The electrochemical measurements were performed in the TMB/H_2O_2 solution. Firstly, the HRP-tagged MBs obtained above were adsorbed on the surface of magnetic-controllable gold working electrode by adding a 2 V voltage on the coil, then, the magnetic-controllable gold working electrode was immersed in 600 μL of TMB/H_2O_2 solution. The cyclic voltammetrys (CVs) or chronoamperometry was carried out with three electrodes system described above. The CVs scanning was performed in the potential range of $0\sim+0.8$ V with a scanning rate of 100 mV/s. The chronoamperometry was performed with incipient potential of $+0.15$ V, the sample interval of 0.1 s and the experimental time of 100 s. The surface temperature of the electrode was detected by infrared thermodetector (Fluke, USA) at the same time.

After electrochemical measurements, the C_p-modified MBs can be revived by dipping the magnetic-controllable gold working electrode into de-ionized water and switching off the power supply of the coil. Without the magnetic field, the MBs were dispersed in the solution again. Then, the solution was incubated at 60 °C for 5 min to dissociate the junction structure on the surface of MBs. As a result, the C_p-modified MBs were revived and can be used for the next cycle of the hybridization and detection.

2.5. The preparation of artificial saliva sample

Un-stimulated saliva samples were collected between 9 a.m. and 10 a.m. with previously established protocols (Navazesh, 1993). Subjects were asked to refrain from eating, drinking, smoking, or oral hygiene procedures for at least 1 h before the collection. Saliva samples were centrifuged at 603 g for 10 min at 4 °C. Then, the 1 mL of supernatant liquid was taken and diluted to 100 mL with hybridization buffer solution. The different concentrations of target miRNA were then added into the diluted saliva to compose artificial saliva samples and the concentrations of target miRNA in the artificial saliva samples were determined with our biosensor.

3. Results and discussion

3.1. Experimental principle of the electrically magnetic-controllable RNA biosensor based on junction probe strategy

As we mentioned above, the electrically magnetic-controllable electrochemical RNA biosensor was fabricated based on a home-made electrically magnetic-controllable gold electrode (see Figure S1 in supporting information) and MBs-based junction-probe strategy. The detailed principle of the proposed biosensor was illustrated in Fig. 1. As shown in Fig. 1, two probes were designed according to "junction-probe" strategy. The first probe is capture probe (C_p, colored black), which was functionalized with a biotin group at one end and then was immobilized on the surface of streptavidin-modified MBs. The second probe is signal probe (S_p, colored green), which was modified with biotin tag at two ends. In the absence of target miRNA (T, colored red), which is a salivary miRNA related to OSCC, C_p and S_p will not hybridize due to the low melting temperature. Whereas, in the presence of target miRNA (T), C_p can hybridize with T and S_p to form a ternary "Y" junction structure on the surface of MBs. The hybrid-attached MBs can capture streptavidin-HRP by the biotinylated S_p. After the capture of streptavidin-HRP, the resulting HRP-tagged MBs have high peroxidase activity and can effectively catalyze the H_2O_2-mediated oxidation of TMB. Then, the HRP-tagged MBs were adsorbed on the surface of the electrically magnetic-controllable working electrode by adding a voltage on the electric coil, and the working electrode was used for electrochemical measurement. Upon dipping the working electrode into the TMB-H_2O_2 solution, the HRP attached on the MBs catalyzed the H_2O_2-mediated oxidation of TMB, which giving rise to an increasing electrochemical current signal. By using this sensing platform, a simple, rapid, ultrasensitive and selective signal-on magnetic-controllable electrochemical biosensor has been developed for the detection of attomolar level OSCC-related miRNA (hsa-miR-200a).

3.2. Optimization of voltage applied to the electrically magnetic-controllable gold electrode

It was well known, the electrified coil not only generate a magnetic field but also generate joule heat. We have studied the influence of the voltage on the magnetic field. We found the magnetic field is strong enough to collect all the functionalized MBs when the voltage is higher than 0.5 V. At the same time, the influence of the voltage on the temperature of the electrode's surface was also investigated. The experimental results indicated that the temperature of the electrode's surface increased when a

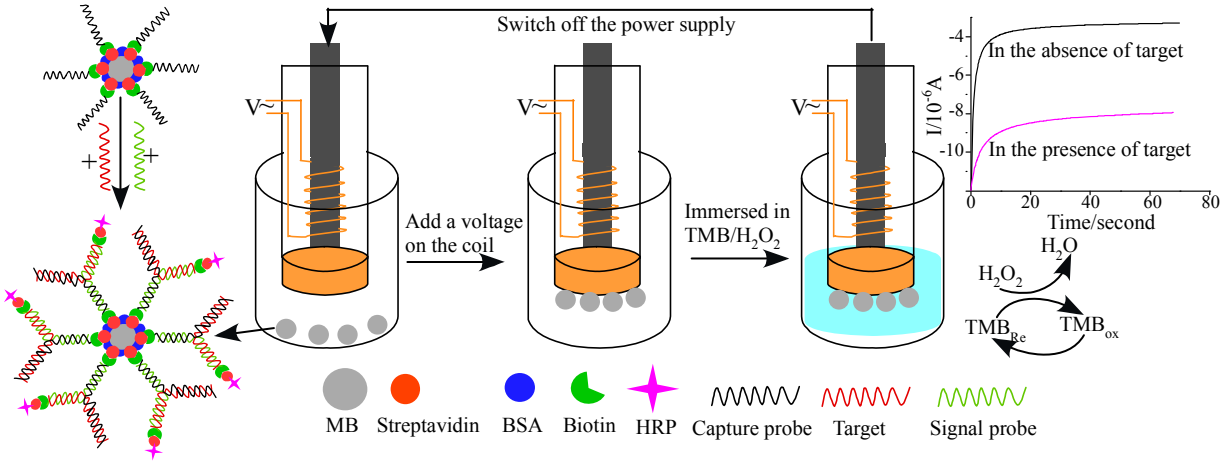

Fig. 1. The principle of the magnetic-controllable electrochemical RNA biosensor.

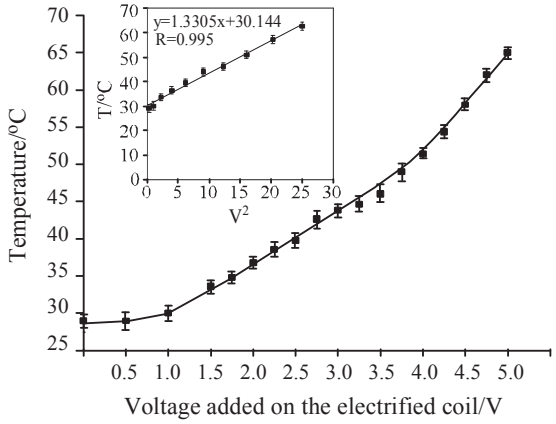

Fig. 2. The relationship of the temperature of the surface of electrically magnetic-controllable gold electrode and the voltage added to the electrified coil.

voltage was added on the coil to generate magnetic field. The temperature of the surface of the working electrode will affect the sensitivity and specificity of the biosensor by affecting the hybridization efficiency of junction structure and the enzymatic activity of the HRP. Fig. 2 showed the relationship between the temperature of the surface of the working electrode and the voltage applied to the coil. From Fig. 2, it was clearly observed that the temperature of the surface of the working electrode rise with the increase of voltage. The temperature showed a good linear relationship with the square of voltage (see insert in Fig. 2), which is the same as that observed in heated electrode (Wei et al., 2009). When the applied voltage is 2 V, the temperature of the electrode's surface is about 37 °C. By considering the fact that the theoretical hybridization temperature of junction structure is about 40 °C (Chen et al., 2008b) and the HRP has the highest enzymatic activity when the temperature to be in the range of 35–38 °C (Tang et al., 2011), 2 V was selected as the optimum voltage.

3.3. Characterization of the magnetic-controllable electrochemical biosensor

The CV behavior of TMB-H_2O_2 was investigated at different stages of the biosensor preparation to validate whether the biosensor actually works as we expected. As shown in Fig. 3A, two pairs of peaks ($E_{p,a1}=+0.28$ V, $E_{p,c1}=+0.34$ V, $E_{p,a2}=+0.44$ V and $E_{p,c2}=+0.49$ V, respectively), which corresponding to two reversible one-electron couples of TMB ($TMB \leftrightarrow TMB^+ + e^-$; $TMB^+ \leftrightarrow TMB^{2+} + e^-$), were observed at the bare gold electrode (Fig. 3A-a) (Doménech et al., 2004). In general, the oxidization of TMB with H_2O_2 is a very slow process. However, in the presence of peroxidase such as HRP, the peroxidase can effectively catalyze the H_2O_2-mediated oxidation of TMB and greatly improve the rate of the oxidation of TMB, which leading to an increasing current signal at $E_{p,a1}$ and $E_{p,c2}$ and a decreasing current signal at $E_{p,c1}$ and $E_{p,a2}$. As shown in Fig. 3A-b, when the C_p-modified MBs are captured on the surface of the gold electrode, there is a little increase in current signal (at $E_{p,a1}$ and $E_{p,c2}$). This should be attributed to the fact that the MBs is of intrinsic peroxidases mimetic activity and can slightly catalyze the H_2O_2-mediated oxidation of TMB (Gao et al., 2007). After C_p-modified MBs hybridized with S_p and T to form "Y" junction structure, and the "Y" junction structure captured the streptavidin-HRP to form HRP-tagged MBs. A highest current signal (at $E_{p,a1}$ and $E_{p,c2}$ respectively) was observed on the surface of the gold electrode, which adsorbed HRP-tagged MBs (Fig. 3A-c). This is because that HRP has high peroxidase activity and can effectively catalyze the

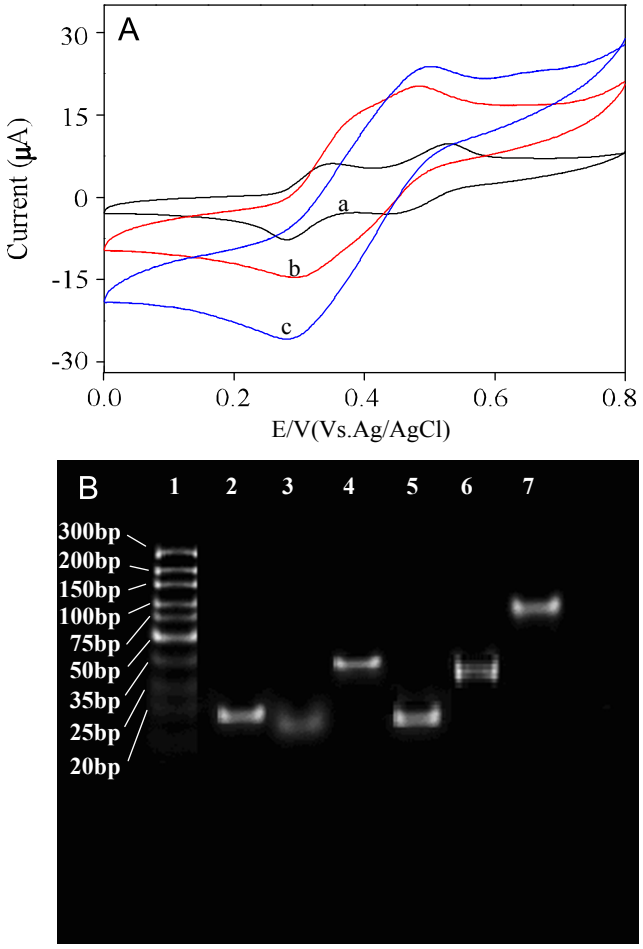

Fig. 3. A: the CVs of TMB-H_2O_2 solution at different electrode's surface. (a) bare magnetic-controllable gold electrode; (b) the magnetic-controllable gold electrode adsorbed C_p-modified MBs; (c) the magnetic-controllable gold electrode adsorbed HRP-tagged MBs. B: The images of polyacrylamide gel electrophoresis (PAGE) experiment. DNA marker (lane 1), C_p (lane 2), S_p (lane3), target miRNA (lane 4), C_p+S_p (lane 5), C_p+target miRNA (Lane 6), C_p+S_p+target miRNA (lane 7). Other conditions: 15% polyacrylamide gels, TBE buffer (0.04 M Tris, 0.04 M H_3BO_3, 1 mM EDTA, pH 8.0).

H_2O_2-mediated oxidation of TMB. At the same time, the solution color observed with the naked eye gradually changed from colorless to blue. The results of CVs indicate that our biosensor indeed works as we expected.

The results of polyacrylamide gel electrophoresis (PAGE) experiment also prove the formation of the "Y" structure. As shown in Fig. 3B, as the expected results, in the absence of target miRNA or signal probe, capture probe can not hybridize with S_p or T to form "Y" junction structure (see lanes 2–6 in Fig. 3B). Whereas, in the presence of both target miRNA and signal probe, capture probe can easily hybridize with S_p and T to form "Y" junction structure (see lane 7 in Fig. 3B), the RNA "Y" structure remained stable in distilled water without dissociating at room temperature (Shu et al., 2011).

3.4. The specificity of the RNA biosensor

The specificity of the proposed RNA biosensor was investigated by detecting various RNA sequences including target miRNA (hsa-miR-200a) and similar miRNAs (hsa-miR-142-3p, hsa-miR-93 and hsa-miR-125a), which are all potential miRNAs identified as being present at statistically significant levels between OSCC patients and healthy controls (Park et al., 2009). As results shown in Fig. 4, in comparison

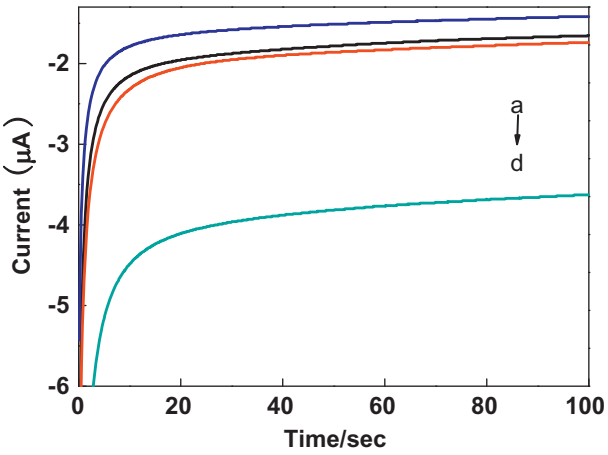

Fig. 4. Current–time curves of C_p-modified MBs after it hybridized with S_p and hsa-miR-142-3p (a), hsa-miR-93 (b), hsa-miR-125a (c) and target miRNA hsa-miR-200a (d) respectively. The concentrations of each miRNA and S_p are all 100 aM.

with target miRNA (curve d), a negligible net current signal was observed for the hsa-miR-142-3p, hsa-miR-93 and hsa-miR-125a respectively (see curves a, b and c in Fig. 4), indicating that similar miRNAs (hsa-miR-142-3p, hsa-miR-93 and hsa-miR-125a) can't hybridize with C_p and S_p to form a stable "Y" junction structure and will not interfere the detection of target miRNA. Higher concentrations of hsa-miR-142-3p, hsa-miR-93 and hsa-miR-125a were also detected to further verify the specificity of our biosensor, and the results showed that 10-fold of similar miRNA do not affect the detection of target miRNA. The experimental result shown in Fig. 4 clearly indicated that the proposed RNA biosensor has an excellent discrimination for similar miRNAs. The high specificity of this biosensor could be attributed to the junction probe strategy and higher surface temperature of magnetic-controllable working electrode (in comparison with general gold electrode).

3.5. The sensitivity of the RNA biosensor

The sensitivity of the proposed RNA biosensor for the detection of target miRNA was investigated by varying the target miRNA concentration. The current signals of TMB/H_2O_2 after the sensor hybridized with different concentration of target miRNA was measured with chronoamperometry (see Fig. 5A). The absolute value of average current shows a good linear correlation with the logarithm of target miRNA concentrations in the range of 1 aM—10 fM (see Fig. 5B). The regression equation is

$$I\ (\mu A) = 0.4608 \times \log C\ (aM) + 3.6962 \quad r = 0.9961$$

The detection limit ($3\sigma/S$, where σ is the standard deviation of the blank solution, $n=8$) was calculated to be 0.22 aM (2.2×10^{-19} M) for complementary target miRNA. The relative standard deviation (RSD) of the biosensor for 8 replicate determination of 0.1 fM target miRNA is 6%.

So far, the magnetic-controllable electrochemical RNA biosensor has not been reported although some magnetic electrochemical DNA biosensors have been developed for the sensitive detection of DNA (Loaiza et al., 2008; Zhang et al., 2013). Loaiza et al. (2008) reported a disposable magnetic electrochemical DNA biosensor, which employed MBs for DNA isolation and hybridization, for the specific detection of DNA related to the enterobacteriaceae family. We also reported a magnetic-controllable electrochemical DNA biosensor for the sensitive detection of DNA related HIV (Zhang et al., 2013). Compared to the existing methods (Loaiza et al., 2008; Zhang et al., 2013), the proposed magnetic-controllable electrochemical RNA biosensor has a much lower detection limit and better specificity. The detection limit of 0.22 aM (2.2×10^{-19} M) is

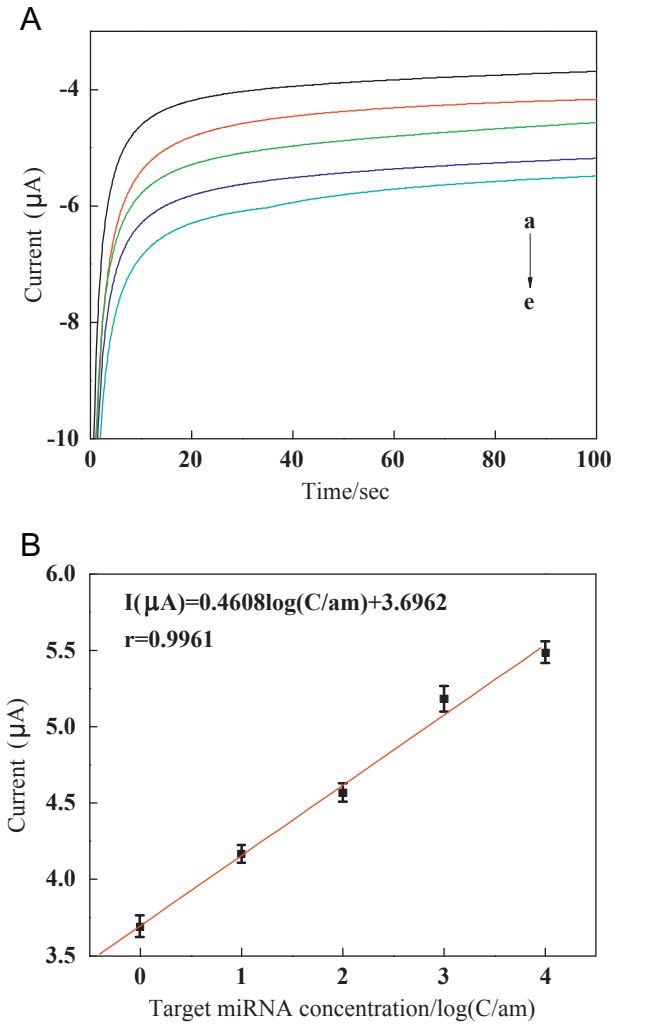

Fig. 5. A: Current–time curves of C_p-modified MBs after it hybridized with different concentration of the target miRNA. From a to e: 1 aM, 10 aM, 100 aM, 1 fM and 10 fM. B: The relationship between current and the logarithm of target miRNA concentrations, which plotted with the data of Fig. 5A.

match to that of PCR-based method. In addition, the disposable magnetic electrochemical biosensor has obvious limitations, for example, the strength and direction of the magnetic field and the temperature of electrode's surface can't be regulated due to the utilization of permanent magnet, the hybridization and detection process was separately performed that makes the biosensor is unsuitable for the on-line analysis, and high analysis cost due to the use of single-used screen printed electrode (Loaiza et al., 2008). In comparison with the previous RNA biosensors (see Table S2 in supporting information), our biosensor has obvious advantages on the sensitivity, specificity, reusability, analysis time and analysis cost due to the utilization of electrically magnetic-controllable gold electrode, MBs-based enzymatic catalysis amplification and junction-probe strategy.

3.6. Detection of saliva sample

In order to evaluate the applicability of our RNA biosensor, the saliva samples spiked with different concentrations of target miRNA were detected with our biosensor. The results shown in Table 1 clearly indicated that the magnetic-controllable electrochemical biosensor has a strong resistance to the complex matrix of saliva, and can be used to detect ultra-trace target miRNA in

Table 1
Determination of target miRNA in artificial saliva sample ($n=5$).

Target miRNA added (aM)	Detected results (aM)	Recovery (%)	RSD (%)
5.0	4.6	93	6
50.0	49.3	99	6
500.0	542.0	108	5

real saliva samples with a recovery of 93-108% and a RSD $< 6\%$ ($n=5$).

4. Conclusions

In summary, we herein first developed a magnetic-controllable electrochemical biosensor for the ultra sensitive and specific detection of oral cancer-related miRNA in saliva based on an electrically magnetic-controllable gold electrode with "junction-probe" strategy and MBs-based enzymatic catalysis amplification. The electrically magnetic-controllable gold electrode combined the merits of heated electrode and magnetic electrode, has notable advantages such as that the strength and direction of the magnetic field and the temperature of the electrode's surface can be easily regulated according to the experimental strategies. These features, as well as the utilization of "junction-probe" strategy and MBs-based enzymatic catalysis amplification, make our biosensor has an ultra-high sensitivity and specificity for the detection of miRNA in real saliva samples. The detection limit of 0.22 aM (2.2×10^{-19} M) is match to that of PCR-based method. The high sensitivity and selectivity, ease of fabrication, operational convenience, short analysis time, better stability and re-usability, make the biosensor a promising alternative for the early point-of-care diagnosis of OSCC.

Acknowledgments

The authors gratefully acknowledge the financial support of NSFC (41240035, 21105012, 21205015), Ministry of Education, Science and Technology Development Center (20123514110001), National Key Technologies R&D Program of China during the 12th Five-Year Plan Period (No. 2012BAD29B06), Program for Changjiang Scholars and Innovative Research Team in University (No. IRT1116), and National Science Foundation of Fujian Province (2012J01035, 2011Y0016).

Appendix A. Supporting information

Supplementary data associated with this article can be found in the online version at http://dx.doi.org/10.1016/j.bios.2013.02.007.

References

Brinkman, B.M., Wong, D.T., 2006. Current Opinion in Oncology 18, 228–233.
Chen, C., Ridzon, D.A., Broomer, A.J., Zhou, Z., Le, D.H., Nguyen, J.T., et al., 2005. Nucleic Acids Research 33, e179.
Chen, J., Lozach, J., Garcia, E.W., Barnes, B., Luo, S., Mikoulitch, I., Zhou, L., Schroth, G., Fan, J.B., 2008a. Nucleic Acids Research 36, e87.
Chen, J.H., Zhang, J., Wang, K., Lin, X.H., Huang, L.Y., Chen, G.N., 2008b. Analytical Chemistry 80, 8028–8034.
Chai, R.L., Grandis, J.R., 2006. Current Treatment Options in Oncology 7, 3–11.
Doménech, A., García, H., Casades, I., Esplá, M., 2004. Journal of Physical Chemistry B 108, 20064–20075.
Fan, C.H., Plaxco, K.W., Heeger, A., 2003. PNAS 100, 9134–9137.
Gao, L.Z., Zhuang, J., Nie, L., Zhang, J.B., Zhang, Y., Gu, N., et al., 2007. Nature Nanotechnology 2, 577–583.
Gao, Z., Peng, Y., 2011. Biosensors and Bioelectronics 26, 3768–3773.
Hu, S., Arellano, M., Boontheung, P., Wang, J.H., Zhou, H., Jiang, J., et al., 2008. Clinical Cancer Research 14, 6246–6252.
Kwon, S.J., Bard, A.J., 2012. Journal of the American Chemical Society 134, 10777–10779.
Liu, C.G., Spizzo, R., Calin, G.A., Croce, C.M., 2008. Methods 44, 22–30.
Loaiza, O.A., Campuzano, S., Pedrero, M., Pividori, M.I., Garcia, P., Pingarron, J.M., 2008. Analytical Chemistry 80, 8239–8245.
Lu, J., Getz, G., Miska, E.A., Alvarez-Saavedra, E., Lamb, J., Peck, D., et al., 2005. Nature 435, 834–838.
Mascini, M., Palchetti, I., Tombelli, S., 2012. Angewandte Chemie International Edition 51, 1316–1332.
Nakayama, S., Yan, L., Sintim, H.O., 2008. Journal of the American Chemical Society 130, 12560–12561.
Navazesh, M., 1993. Annals of the New York Academy of Sciences 694, 72–77.
Park, N., Zhou, H., Elashoff, D., Henson, B.S., Kastratovic, D.A., Abemayor, E., Wong, D.T., 2009. Clinical Cancer Research 15, 5473–5477.
Peng, Y., Gao, Z., 2011. Analytical Chemistry 83, 820–827.
Raymond, C.K., Roberts, B.S., Garrett-Engele, P., Lim, L.P., Johnson, J.M., 2005. RNA 11, 1737–1744.
Shu, D., Shu, Y., Haque, F., Abdelmawla, S., Guo, P.X., 2011. Nature Nanotechnology 6, 658–667.
Tang, Z., Wu, H., Zhang, Y., Li, Z., Lin, Y., 2011. Analytical Chemistry 83, 8611–8616.
Válóczi, A., Hornyik, C., Varga, N., Burgyan, J., Kauppinen, S., Havelda, Z., 2004. Nucleic Acids Research 32, e175.
von Lode, P., 2005. Clinical Biochemistry 38, 591–606.
Warsinke, A., 2009. Analytical and Bioanalytical Chemistry 393, 1393–1405.
Wei, H., Sun, J.J., Guo, L., Li, X., Chen, G.N., 2009. Chemical Communication 20, 2842–2844.
Zetola, N.M., Pilcher, C.D., 2007. Infectious Disease Clinics of North America 21, 19–48.
Zhang, J., Chen, J.H., Chen, R.C., Chen, G.N., Fu, F.F., 2009. Biosensors and Bioelectronics 25, 815–819.
Zhang, J., Wu, X.Y., Chen, P.P., Lin, N.T., Chen, J.H., Chen, G.N., Fu, F.F., 2010. Chemical Communication 46, 6986–6988.
Zhang, J., Wu, X.Y., Yang, W.J., Chen, J.H., Fu, F.F., 2013. Chemical Communication 49, 996–999.